^{100}Sn-daughter α-nuclei cluster decays of some neutron-deficient Xe to Gd parents: Sn radioactivity

Satish Kumar, Dharam Bir,* and Raj K. Gupta
Physics Department, Panjab University, Chandigarh-160014, India
(Received 18 May 1994)

Cluster decays of the neutron-deficient $^{108-116}$Xe, $^{112-120}$Ba, $^{116-124}$Ce, $^{120-124}$Nd, $^{124-128}$Sm, and $^{128-132}$Gd parents are studied within the preformed cluster model of Malik and Gupta. The calculated preformation probabilities (P_0) and decay half-lives show that the α-nuclei ($A_2 = 4n$, $Z_2 = N_2$) clusters, like ^{8}Be, ^{12}C, ^{16}O, ^{20}Ne, ^{24}Mg, and ^{28}Si, emitted from $N = Z$ parents are the most probable cases for measurements. Many of these clusters are shown to be within the upper limit of present experimental methods. This stresses the importance of $^{100}_{50}$Sn-daughter in these decays. The fact that $A_2 = 4n$ cluster decays are more probable than $A_2 = 4n+2$ clusters demonstrates that Sn radioactivity is associated with $A_2 = 4n$, $Z_2 = N_2$ (α-nuclei) clusters. Structure effects of the nuclear (proximity) potential and binding energies (the shell effects) in GN plots and in variation of P_0 with the parent mass A are also pointed out.

PACS number(s): 23.60.+e, 27.60.+j, 23.90.+w, 21.60.Gx

I. INTRODUCTION

Cluster decay of a $N = Z$, $A = 4n$ nucleus via α nuclei ($A_2 = 4n$, $Z_2 = N_2$) clusters was first pointed out in 1988 by Gupta and collatorators [1]. For very light nuclei ($A \leq 80$), it was shown that the minima in potential energy surfaces lie always and only at α nuclei. As the neutron-proton ratio N/Z becomes larger than one, other clusters of the type observed in the decay of radioactive nuclei also start appearing and become equally predominant for $N/Z \gg 1$ parents. More recently [2,3], the same kind of instability was predicted explicitly for decays of Ba isotopes, which has now been observed experimentally, first by Tretyakova *et al.* [4] at Dubna (Russia) and more recently[1] by Guglielmetti *et al.* [5] at GSI, Darmstadt (Germany). The α nuclei ^{4}He, ^{8}Be, ^{12}C, ^{16}O, and ^{20}Ne were predicted [3] as the possible decay modes of $^{112-120}$Ba, observable with the presently available experimental methods. Other than the α particle, ^{12}C decay of ^{112}Ba was predicted to be the best candidate for experiments, with decay half-life $T_{1/2}(^{12}\mathrm{C})=5.62 \times 10^3$ s, which depends strongly on the Q-value estimate. For ^{12}C decay of ^{114}Ba, the calculated [3] $T_{1/2}(^{12}\mathrm{C})=1.32\times10^5 - 4.68 \times 10^9$ s for different Q values, to be compared with the recently measured [5] $T_{1/2}(^{12}C) \sim 1.7 \times 10^4$ s. For α decay of ^{114}Ba, the measured $T_{1/2}(\alpha) > 500$ s, which is to be compared with the predicted [3] $T_{1/2}(\alpha) = 9.12 \times 10^4$ s. It may be recalled here that, in general, the predicted half-life times for α decays in the model of Malik and Gupta [1,6] are underestimated. The collective desription is not expected to give a proper description of α decay. In view of this fact, already considered by Malik and Gupta [6], instead of the branching ratios, the calculated half-lives for heavy cluster decays are more relevant here, and we follow the same spirit in this paper. The calculated branching ratios of Malik and Gupta [6] for heavy cluster decays of radioactive nuclei are known (see Table III in Ref. 6) to be good within two to three orders of magnitude due to their poor estimation of α decay half-lives by about the same orders of magnitude. However, the calculated half-lives for heavy cluster decays in this model [6] match within less than one order of magnitude with the early microscopic calculations of Blendowske *et al.* [7] for the observed ^{14}C decay of Ra isotopes and with a very recent[2] fully microscopic calculation of Delion *et al.* [8] for ^{12}C decay of ^{114}Ba (compare $\log_{10}T_{1/2}(\mathrm{s})$=5.12 of Ref. [3] with $\log_{10}T_{1/2}(\mathrm{s})$=5.02 of Ref. [8]; notice that the Q values are slightly different in the two cases).

The above study is extended by some authors [9,10] to many neutron-deficient isotopes of $_{57}$La, $_{58}$Ce, $_{60}$Nd, and $_{62}$Sm parents, predicting many new $A_2 = 4n$ cluster decays. In this paper, we extend our own study of Refs. [2] and [3] to many neutron-deficient isotopes of $_{54}$Xe to $_{64}$Gd nuclei, which can be produced in the laboratory by using the radioactive beams. The case of $_{56}$Ba parents, studied in Ref. [3], is also included here in the discussion of our results. The interesting aspect of this study is the existence of a spherical, doubly closed shell, $^{100}_{50}$Sn-daughter for $A_2 = 4n$, $Z_2 = N_2$ clusters $^{8}_{4}$Be to $^{28}_{14}$Si. The predicted half-lives for many of these most favorable cases are $\sim 10^3$ to 10^{12} s, which are far below the present experimental limit of measurements. We have used here the preformed cluster model (PCM) of Malik and Gupta [1,6], where the cluster preformation proba-

*Permanent address: Physics Department, Kurukshetra University, Kurukshetra (Haryana), India.

[1]This result became available only at the time of revising this manuscript.

[2]See footnote 1.

bility is the quantum mechanical formation yield based on collective model picture of the nucleus. This PCM has now been used extensively [2,3,11–15] and is perhaps the only theoretical prescription so far available for calculating the cluster preformation probability, other than the early shell model description of Blendowske *et al.* [7] and more recently of Delion *et al.* [8]. For a recent review of these models, we refer the reader to Ref. [16].

Section II gives a brief description of the preformed cluster model [6]. Our calculations and discussion of results are presented in Sec. III. Finally, a summary of our conclusions is given in Sec. IV.

II. THE MODEL

The decay half-life $T_{1/2}$ or the decay constant λ in a preformed cluster model is defined as

$$\lambda = P_0 \nu_0 P \quad (T_{1/2} = \ln 2/\lambda) \ . \tag{1}$$

Here, P_0 is the cluster preformation probability, ν_0, the barrier impinging frequency (s^{-1}) and P, the barrier penetration probability. Malik and Gupta [6] considered the solving of the following stationary Schrödinger equation for a coupled motion in dynamical collecitve coordinates of mass asymmetry $\eta = (A_1 - A_2)/A$, with $A = A_1 + A_2$, and relative separation R:

$$H(\eta, R)\psi^m(\eta, R) = E^m \psi^m(\eta, R) \ , \tag{2}$$

with the Hamiltonian constructed as

$$H(\eta, R) = V(\eta) + V(R) + V(\eta, R) + \tfrac{1}{2} B_{\eta\eta} \dot{\eta}^2 + \tfrac{1}{2} B_{RR} \dot{\vec{R}}^2 + \vec{B}_{\eta R} \dot{\eta} \dot{\vec{R}} \ . \tag{3}$$

The charges Z_i $(i = 1, 2)$ of fragments are fixed by minimizing the potential in an equivalent charge asymmetry coordinate $\eta_Z = (Z_1 - Z_2)/Z$. The energies E^m $(m = 0, 1, 2, 3, \ldots)$ give the energy spectrum of the system in the potential $V(\eta, R)$. The nature of this spectrum will apparently depend on the shape of the system which is specified by the collective coordinates of relative separation R and the mass asymmetry η. For cluster radioactivity, $|\eta|$ is very large, close to unity. For such a nuclear shape, the η motion corresponds mainly to octupole oscillations. Hence, the calculated energies E^m could be said to refer to octupole states of the cluster-core system, and these states usually lie higher in energies. Actually, cluster-core models for low lying energy spectra (and other nuclear properties) are expected to be good only for light nuclei [17,18], where the mass asymmetry η is not too large. Within the semimicroscopic algebraic approach, one of us and collaborators [19] have been able to overcome this difficulty of asymmetricity in η motion by introducing antisymmetrization effects of wave functions in the very asymmetric clusterization of heavy nuclei. The low-lying bands calculated for the cluster-core configuration ^{14}C+^{210}Pb compare nicely with the experimental energy spectrum of ^{224}Ra.

In actual practice, the above problem reduces to one of the decoupled motions since, for collective potentials calculated in Strutinsky method and B_{ij} as cranking masses, both the coupling potential $V(\eta, R)$ and coupling mass $B_{\eta R}$ are small [20–23]. Then, $\psi^m(\eta, R) = \psi^m(\eta)\psi^m(R)$, $E^m = E^m_\eta + E^m_R$, with $P_0 \propto |\psi^m(\eta)|^2$ and $P \propto |\psi^m(R)|^2$. We use here only the ground state $(m = 0)$ solutions, since the cluster-decay is considered to occur in the ground-state of the daughter nucleus.

For the η motion, the stationary Schrödinger equation (2) becomes

$$\left(-\frac{\hbar^2}{2\sqrt{B_{\eta\eta}}} \frac{\partial}{\partial \eta} \frac{1}{\sqrt{B_{\eta\eta}}} \frac{\partial}{\partial \eta} + V(\eta) \right) \psi^m(\eta) = E^m_\eta \psi^m(\eta) \ , \tag{4}$$

whose (numerical) solutions for fixed R give the fractional cluster preformation probabilities (in the ground-state $m = 0$)

$$P_0(A_2) = |\psi^0(\eta)|^2 \sqrt{B_{\eta\eta}(\eta)} \frac{2}{A} \ . \tag{5}$$

The value of R is taken as the inner turning point $R_a = R_1 + R_2$ $(= R_t)$ or $= C_1 + C_2 (= C_t)$, C_i being the Süssmann central radii [24], and the potential $V(\eta)$ for such a two touching spheres approximation is given as the sum of nuclear binding energies, the Coulomb and the proximity [25] potentials. The masses $B_{\eta\eta}$ $(\equiv B_{\xi\xi})$ are the classical hydrodynamical masses of Kröger and Scheid [26], where ξ is, equivalently, the volume asymmetry coordinate ($\eta = \xi$ under constant density approximation).

In Eq. (4), E^m_η are the energies of the cluster-core system in potential $V(\eta)$ at $R = R_t$. In the presence of coupling between R and η motions, these energies due to the η degree of freedom are different for different values of R and, say, for ground state decay E^0_η should be added to the scattering potential $V(R)$. Notice that the mass parameters $B_{\eta\eta}$, which implies mass transfer, also contribute towards the determination of E^m_η. The microscopic Cranking masses [20,21] $B_{\eta\eta}$ show strongly peaked behavior (almost like δ function) at η values referring to physical transfer of masses. Thus at specific η values, the probabilities P_0 get enhanced considerably and the energies E^m_η become very large. In the present calculations, however, we have used the smoothly varying hydrodynamical masses $B_{\xi\xi}$ and further assumed that E^m_η remain constant in R degree of freedom. For ^{12}C decay of ^{114}Ba at $R = R_t$, for example, $E^0_\eta = 13.87$ MeV which is the zero-point vibrational energy of the collective η motion, to be added to the zero-point vibrational energy E^0_R of the collective R motion (discussed below). The first excited state $(E^1_\eta - E^0_\eta)$ is calculated to be 4.01 MeV, which is interpreted as an octupole vibrational state in potential $V(\eta)$ of ^{114}Ba (Fig. 1).

For the R motion, instead of solving the corresponding radial Schrödinger equation, as usual Malik and Gupta [6] used the WKB approximation and calculated P analytically by parametrizing $V(R)$ suitably for each η (and η_Z) and for $R \geq R_t$ or C_t. For the penetration path shown in Fig. 1 of Ref. [6], and assuming, for simplicity,

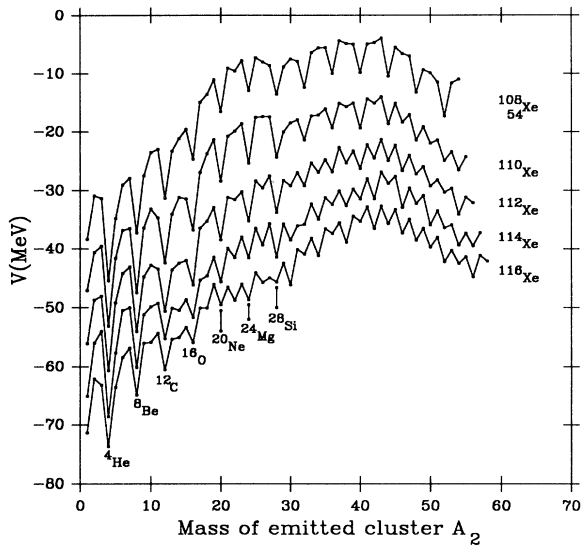

FIG. 1. Fragmentation potentials for $^{108-116}$Xe parents, at $R_a = C_1 + C_2$.

the internal deexcitation probability $W_i = 1$, the barrier penetrability

$$P = P_i P_b \ , \tag{6}$$

with the WKB penetrabilities

$$P_i = \exp\left(-\frac{2}{\hbar}\int_{R_t}^{R_i}[2\mu\{V(R) - V(R_i)\}]^{1/2}dR\right) \ , \tag{7}$$

$$P_b = \exp\left(-\frac{2}{\hbar}\int_{R_i}^{R_b}[2\mu\{V(R) - Q\}]^{1/2}dR\right) \ . \tag{8}$$

Here, R_i is defined by $V(R_i) = V(R_a)$ with $V(R_a) = V(R_t) = Q + E_i$. E_i is the energy that was considered [6] to represent the decay into the excited states of the daughter nucleus (or the cluster or both). An internal deexcitation probability W_i was introduced that scale exponentially with E_i. For heavy cluster decays $W_i = 1$, as already stated above. Recently, Kumar and Gupta [27,28] have shown that these phenomenological effects of taking $R_a = R_t$ and introducing the idea of internal deexcitation in the model of Malik and Gupta compensate for the neglected deformation effects of both the cluster and daughter nuclei. Inclusion of deformations of both the cluster and daughter nuclei lowers down the barrier considerably with the inner turning point R_a ($> R_0$, R_0 is the equivalent spherical radius of the parent nucleus) lying at the Q value. R_b is the outer turning point with $V(R_b) = Q$ value of the decay process.

The impinging frequency ν_0 in Eq. (1) is defined simply as

$$\nu_0 = \frac{v}{R_0} = \frac{\sqrt{2Q/mA_2}}{R_0} \ , \tag{9}$$

where mA_2 is the mass of the emitted cluster. Apparently, here the total kinetic energy, shared between the two fragments, is the positive Q value. Alternatively, ν_0 can be calculated [29,16] by parametrizing $V(R)$ around the parent nucleus radius R_0 to an harmonic oscillator (see, e.g., Fig. 1 in Ref. [6]). This would also require the mass parameter B_{RR} in R degree of freedom, which is usually taken as the reduced mass (see Ref. [16] for details). The two methods, however, give a similar result, which is further illustrated below for the case of ^{12}C decay of ^{114}Ba.

The quantity ν_0 represents the zero-point vibrational energy $E_R^0 (= \frac{1}{2}\hbar\omega = \frac{1}{2}h\nu_0)$ due to relative motion R, and can be compared with, say, the empirical estimates of Poenaru *et al.* [30] for their so-called $E_{\rm vib}$ (see, e.g., Eq. (3) in Ref. [6]). For ^{12}C decay of ^{114}Ba, we get $E_R^0 = 6.68$ MeV by using Eq. (9) and 4.13 MeV for the alternative procedure [29,16] of approximating the potential $V(R_0 \le R \le R_t)$ by an harmonic oscillator. Using the empirical formula of Poenaru *et al.* [30] $E_{\rm vib} = 1.16$ MeV for ^{12}C decay of ^{114}Ba which is lower by a factor of 2 to 4 than the above-mentioned two theoretical estimates. Notice that E_R^0 (or $E_{\rm vib}$) is much smaller compared to E_η^0 and that this factor of 2 to 4 difference in E_R^0 and $E_{\rm vib}$ results in a change of ν_0 value by the same factor, which is not very significant because the order of estimated half-life times does not change. In our case the total zero-point vibrational energy is $E^0 = E_\eta^0 + E_R^0$, which must be added to the Q value for the penetrability calculation. Remember, however, that E_η^0 would enter the calculation only if its contributions at all R values are added to the scattering $V(R)$, as already discussed above. In any case, E^0 does not enter into our calculations because we have defined our inner turning point by $V(R_a) = V(R_t)$, rather than equal to $Q + E_R^0$ (E_η^0 is taken to be constant, independent of R). For the ^{12}C decay of ^{114}Ba, the two quantities are nearly the same (compare $V(R_t) = 25.96$ MeV with $Q + E_R^0 = 26.88$ MeV). This means that our inner turning point $R_a = R_t$ lies nearly at the zero point vibrational energy E_R^0, above the Q value.

III. CALCULATIONS

First of all, we look at the static fragmentation potentials V as a function of cluster mass A_2. This is illustrated in Fig. 1 for $^{108-116}_{54}$Xe parents. We concentrate here only on the potential energy minima, since the preformation probabilities P_0 for clusters referring to minima are always larger compared to their neighboring clusters [31]. We notice that for the $N = Z$ nucleus (here ^{108}Xe), in agreement with earlier works of Refs. [1] and [3], the potential energy minima occur only at $A_2 = 4n$ α nuclei. We shall see in the following that cluster-decay constant λ is largest (or the decay half-life $T_{1/2}$ smallest) for such a highly neutron deficient parent to decay with a $A_2 = 4n$, $Z_2 = N_2$ cluster referring to doubly magic $Z_1 = N_1 = 50$ ^{100}Sn daughter. As the neutron-proton ratios N/Z of the parent nuclei increase, the potential energy minima at $A_2 = 4n + 2$ clusters also start appearing. For $N \gg Z$ parents (see, e.g., ^{114}Xe or ^{116}Xe), some of the minima at $A_2 = 4n + 2$ are as deep as at $A_2 = 4n$ clusters. In the following, we discuss our cal-

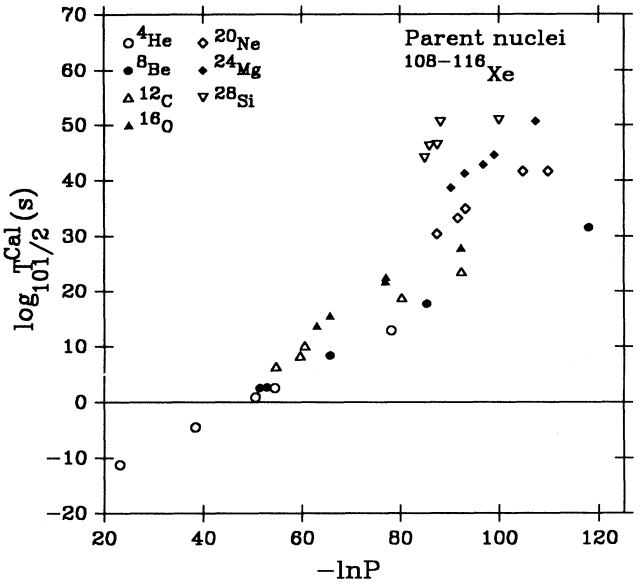

FIG. 2. Geiger-Nuttall plots of $\log_{10} T^{\rm cal}_{1/2}$ (s) vs $-\ln P$ for various clusters emitted from $^{108-116}$Xe.

culations of the dynamical cluster-decay process for both the $A_2 = 4n$ and $4n + 2$ clusters, though the present experiments are directed more towards the more exotic, and highly probable $A_2 = 4n$ (α nuclei) decays of $Z = N$ parents.

A. $A_2 = 4n$ cluster decays

We have first analyzed the Geiger-Nuttall (GN) plots for all the parents. In each case, the structure effects of nuclear proximity potential or the binding energies (the shell effects) are evident. This is illustrated in Figs. 2 and 3 for Xe isotopes. The $\log_{10} T^{\rm cal}_{1/2}$(s) vs $-\ln P$ plots in Fig. 2 show the role of nuclear (proximity) potential in terms of differences in slopes and small deviations from straight lines (the GN law is an equation of straight line for P as the pure Coulomb barrier penetrability). Similarly, Fig. 3 shows that $\log_{10} T^{\rm cal}_{10}$(s) vs $Q^{-1/2}$ plots represent different GN laws (the equations of straight lines) for different clusters, which is associated [3] with each cluster having a different preformation factor P_0. This later result is demonstrated in Fig. 4 for Xe and Ce parents. We notice that ^{4}He is always preformed with the largest probability (smallest $-\log_{10} P_0$ value) and,

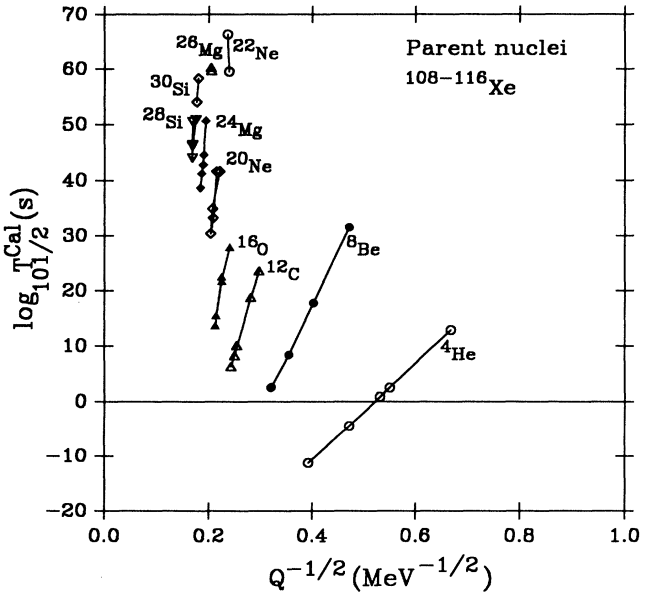

FIG. 3. Geiger-Nuttall plots of $\log_{10} T^{\rm cal}_{1/2}$ (s) vs $Q^{-1/2}$ for various clusters emitted from $^{108-116}$Xe.

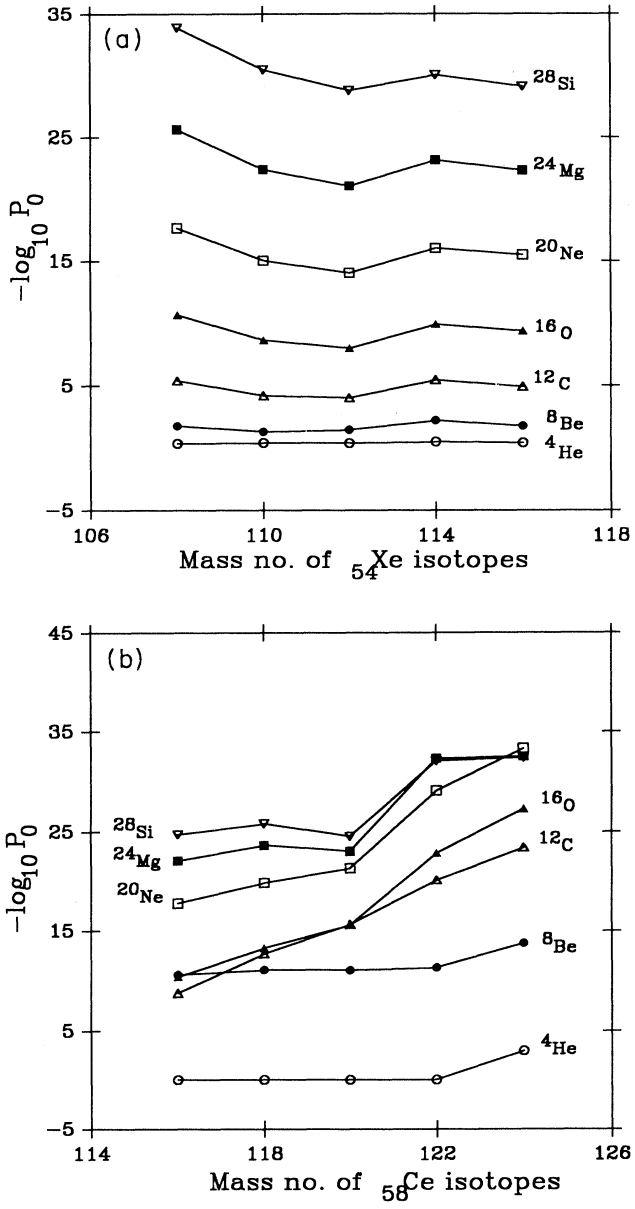

FIG. 4. (a) Logarithm of cluster preformation probability P_0 vs mass of parent nuclei $^{108-116}$Xe, for the emission of different clusters; (b) Same as in Fig. 4(a), but for $^{116-124}$Ce.

TABLE I. Predicted half-lives $T_{1/2}$ (s) and other characteristics for cluster decays of some neutron deficient parents from Xe to Gd. For Q-value estimates the masses for Xe to Nd parents are taken from Möller and Nix [32] for $A \geq 16$ and Wapstra *et al.* [32] for $A < 16$ (except other wise stated) and for Sm and Gd parents from Comey *et al.* [32] and Wapstra *et al.* [32].

Parent nucleus	Emitted cluster	Daughter nucleus	Q value (MeV)	Preformation probability P_0	Decay constant λ (s^{-1})	$\log_{10} T^{cal}_{1/2}$ (s) Present	Ref. [9]	Ref. [10]
^{108}Xe	^{4}He	^{104}Te	6.49	4.40×10^{-1}	1.25×10^{11}	−11.26		
	^{8}Be	^{100}Sn	9.77	1.70×10^{-2}	2.20×10^{-3}	2.50		
	^{12}C	^{96}Cd	15.45	3.74×10^{-6}	5.44×10^{-11}	10.11		
	^{16}O	^{92}Pd	19.71	2.06×10^{-11}	1.94×10^{-23}	22.55		
	^{20}Ne	^{88}Ru	21.56	2.13×10^{-18}	1.67×10^{-42}	41.62		
	^{24}Mg	^{84}Mo	26.58	2.31×10^{-26}	1.49×10^{-51}	50.67		
	^{28}Si	^{80}Zr	35.00	1.40×10^{-34}	2.06×10^{-51}	50.53		
^{110}Xe	^{4}He	^{106}Te	4.49	4.00×10^{-1}	2.11×10^{4}	−4.48		
	^{8}Be	^{102}Sn	9.71	4.91×10^{-2}	1.51×10^{-3}	2.66		
	^{12}C	^{98}Cd	16.88	6.25×10^{-5}	3.26×10^{-7}	6.33		
	^{16}O	^{94}Pd	21.74	2.14×10^{-9}	1.87×10^{-16}	15.57		
	^{20}Ne	^{90}Ru	23.19	9.02×10^{-16}	3.70×10^{-34}	33.27		
	^{24}Mg	^{86}Mo	28.88	3.79×10^{-23}	3.89×10^{-42}	41.25		
	^{28}Si	^{82}Zr	35.55	3.69×10^{-31}	4.83×10^{-47}	46.16		
^{112}Xe	^{4}He	^{108}Te	3.31	4.10×10^{-1}	2.01×10^{-3}	2.54		
	^{8}Be	^{104}Sn	7.95	3.56×10^{-2}	2.79×10^{-9}	8.40		
	^{12}C	^{100}Cd	15.96	9.27×10^{-5}	3.67×10^{-9}	8.28		
	^{16}O	^{96}Pd	22.19	9.30×10^{-9}	1.23×10^{-14}	13.75		
	^{20}Ne	^{92}Ru	24.17	9.10×10^{-15}	2.68×10^{-31}	30.41		
	^{24}Mg	^{88}Mo	29.43	8.47×10^{-22}	1.43×10^{-39}	38.69		
	^{28}Si	^{84}Zr	35.55	1.76×10^{-29}	6.36×10^{-45}	44.04		
^{114}Xe	^{4}He	^{110}Te	3.35	3.30×10^{-1}	8.63×10^{-2}	0.90		
	^{8}Be	^{106}Sn	6.18	6.30×10^{-3}	1.13×10^{-18}	17.79		
	^{12}C	^{102}Cd	12.70	3.29×10^{-6}	1.13×10^{-19}	18.79		
	^{16}O	^{98} Pd	19.71	1.16×10^{-10}	1.22×10^{-22}	21.76		
	^{20}Ne	^{94}Ru	23.29	9.40×10^{-17}	8.16×10^{-36}	34.93		
	^{22}Ne	^{92}Ru	17.55	3.07×10^{-20}	2.19×10^{-60}	59.50		
	^{24}Mg	^{90}Mo	27.77	6.66×10^{-24}	1.77×10^{-45}	44.59		
	^{26}Mg	^{88}Mo	24.11	9.03×10^{-28}	3.80×10^{-61}	60.26		
	^{28}Si	^{86}Zr	35.09	1.00×10^{-30}	2.64×10^{-47}	46.42		
^{116}Xe	^{4}He	^{112}Te	2.24	4.00×10^{-1}	8.79×10^{-14}	12.99		
	^{8}Be	^{108}Sn	4.50	1.73×10^{-2}	1.91×10^{-32}	31.56		
	^{12}C	^{104}Cd	11.32	1.15×10^{-5}	1.93×10^{-24}	23.55		
	^{16}O	^{100}Pd	17.35	3.87×10^{-10}	8.19×10^{-29}	27.93		
	^{20}Ne	^{96}Ru	20.51	3.20×10^{-16}	1.62×10^{-42}	41.63		
	^{22}Ne	^{94}Ru	17.99	1.43×10^{-19}	3.10×10^{-67}	66.35		
	^{24}Mg	^{92}Mo	28.13	4.58×10^{-23}	1.10×10^{-43}	42.80		
	^{26}Mg	^{90}Mo	23.77	9.38×10^{-27}	1.33×10^{-60}	59.72		
	^{28}Si	^{88}Zr	32.51	8.38×10^{-30}	8.64×10^{-52}	50.90		
^{116}Ce	^{4}He	^{112}Ba	3.09	9.97×10^{-1}	4.94×10^{-7}	6.15		
	^{8}Be	^{108}Xe	7.32	2.53×10^{-11}	2.09×10^{-24}	23.52		
	^{12}C	^{104}Te	21.17	1.73×10^{-9}	4.38×10^{-7}	6.20		
	^{16}O	^{100}Sn	31.71	4.23×10^{-11}	5.06×10^{-7}	6.14		
	^{20}Ne	^{96}Cd	34.76	1.66×10^{-18}	1.45×10^{-20}	19.68		
	^{24}Mg	^{92}Pd	41.16	7.87×10^{-23}	1.07×10^{-26}	25.81		
	^{28}Si	^{88}Ru	48.26	1.80×10^{-25}	1.45×10^{-28}	27.68		
^{118}Ce	^{4}He	^{114}Ba	2.58	9.97×10^{-1}	6.34×10^{-12}	11.04		
	^{8}Be	^{110}Xe	5.61	8.38×10^{-12}	2.27×10^{-36}	35.48		
	^{12}C	^{106}Te	17.46	2.03×10^{-13}	2.38×10^{-17}	16.47		
	^{16}O	^{102}Sn	29.94	5.29×10^{-14}	1.13×10^{-11}	10.79	11.0	9.6[a]
	^{20}Ne	^{98}Cd	34.48	1.40×10^{-20}	3.05×10^{-23}	22.36		
	^{24}Mg	^{94}Pd	41.53	2.24×10^{-24}	2.81×10^{-27}	26.39		
	^{28}Si	^{90}Ru	48.18	1.55×10^{-26}	2.17×10^{-29}	28.50		

TABLE I. (*Continued*).

Parent nucleus	Emitted cluster	Daughter nucleus	Q value (MeV)	Preformation probability P_0	Decay constant λ (s^{-1})	$\log_{10} T^{cal}_{1/2}$ (s) Present	Ref. [9]	Ref. [10]
^{120}Ce	^{4}He	^{116}Ba	2.33	9.98×10^{-1}	7.23×10^{-14}	12.98		
	^{8}Be	^{112}Xe	4.55	9.06×10^{-12}	6.76×10^{-50}	49.01		
	^{12}C	^{108}Te	15.19	2.21×10^{-16}	5.84×10^{-26}	25.08		
	^{16}O	^{104}Sn	27.12	2.63×10^{-16}	1.12×10^{-17}	16.79	16.6	14.0[b]
	^{20}Ne	^{100}Cd	32.50	4.57×10^{-21}	1.06×10^{-27}	26.82		
	^{24}Mg	^{96}Pd	40.87	9.17×10^{-24}	2.20×10^{-27}	26.50		
	^{28}Si	^{92}Ru	48.10	2.98×10^{-25}	2.22×10^{-28}	27.50		
^{122}Ce	^{4}He	^{118}Ba	2.09	9.96×10^{-1}	1.27×10^{-15}	14.74		
	^{8}Be	^{114}Xe	3.89	5.11×10^{-12}	3.01×10^{-56}	55.36		
	^{12}C	^{110}Te	14.80	7.75×10^{-21}	1.88×10^{-31}	30.57		
	^{16}O	^{106}Sn	24.69	1.39×10^{-23}	5.90×10^{-29}	28.07	21.9	20.1[b]
	^{20}Ne	^{102}Cd	28.58	8.13×10^{-30}	4.87×10^{-42}	41.15		
	^{22}Ne	^{100}Cd	26.38	7.84×10^{-33}	7.27×10^{-51}	49.98		
	^{24}Mg	^{98}Pd	37.73	4.99×10^{-33}	2.56×10^{-41}	40.43		
	^{26}Mg	^{96}Pd	34.89	6.66×10^{-34}	1.13×10^{-47}	46.79		
	^{28}Si	^{94}Ru	46.56	8.85×10^{-33}	3.67×10^{-38}	37.28		
^{124}Ce	^{4}He	^{120}Ba	1.73	9.90×10^{-4}	2.31×10^{-22}	21.48		
	^{8}Be	^{116}Xe	3.17	1.79×10^{-14}	6.53×10^{-67}	66.03		
	^{12}C	^{112}Te	12.77	3.86×10^{-24}	1.19×10^{-41}	40.77		
	^{16}O	^{108}Sn	22.26	5.24×10^{-28}	2.85×10^{-38}	37.39	27.9	27.0[b]
	^{20}Ne	^{104}Cd	26.53	4.93×10^{-34}	5.38×10^{-51}	50.11		
	^{22}Ne	^{102}Cd	26.10	9.69×10^{-36}	9.60×10^{-55}	53.86		
	^{24}Mg	^{100}Pd	34.65	3.18×10^{-33}	8.99×10^{-47}	45.89		
	^{26}Mg	^{98}Pd	33.01	1.01×10^{-30}	7.71×10^{-48}	46.95		
	^{28}Si	^{96}Ru	43.06	4.31×10^{-33}	1.42×10^{-42}	41.69		
^{120}Nd	^{4}He	^{116}Ce	3.03	9.96×10^{-1}	1.43×10^{-7}	6.69		
	^{8}Be	^{112}Ba	6.02	6.03×10^{-12}	5.77×10^{-36}	35.08		
	^{12}C	^{108}Xe	17.71	1.14×10^{-16}	1.04×10^{-21}	20.83		
	^{16}O	^{104}Te	31.36	1.79×10^{-15}	8.67×10^{-13}	11.90		
	^{20}Ne	^{100}Sn	39.41	1.99×10^{-19}	6.26×10^{-18}	17.04		
	^{24}Mg	^{96}Cd	47.09	1.25×10^{-22}	1.02×10^{-21}	20.83		
	^{28}Si	^{92}Pd	54.17	3.95×10^{-25}	1.20×10^{-24}	23.76		
^{122}Nd	^{4}He	^{118}Ce	2.95	9.97×10^{-1}	1.93×10^{-8}	7.56		
	^{8}Be	^{114}Ba	5.43	1.18×10^{-11}	1.38×10^{-40}	39.70		
	^{12}C	^{110}Xe	15.92	1.33×10^{-16}	1.82×10^{-26}	25.58		
	^{16}O	^{106}Te	22.57	1.36×10^{-17}	5.26×10^{-21}	20.12	23.0[c]	16.4[a]
	^{20}Ne	^{102}Sn	37.62	4.41×10^{-19}	1.42×10^{-19}	18.69		
	^{24}Mg	^{98}Cd	46.76	2.36×10^{-20}	1.16×10^{-19}	18.78		
	^{28}Si	^{94}Pd	54.41	6.37×10^{-22}	6.90×10^{-21}	20.00		
^{124}Nd	^{4}He	^{120}Ce	2.81	9.97×10^{-1}	1.34×10^{-9}	8.71		
	^{8}Be	^{116}Ba	5.04	1.04×10^{-11}	1.21×10^{-44}	43.76		
	^{12}C	^{112}Xe	14.72	3.55×10^{-20}	1.36×10^{-33}	32.71		
	^{16}O	^{108}Te	25.16	1.48×10^{-22}	2.25×10^{-29}	28.49		
	^{20}Ne	^{104}Sn	34.66	1.08×10^{-24}	5.90×10^{-29}	28.07		
	^{24}Mg	^{100}Cd	44.61	4.76×10^{-25}	1.63×10^{-26}	25.63		
	^{28}Si	^{96}Pd	53.66	3.43×10^{-25}	9.30×10^{-25}	23.87		
^{124}Sm	^{4}He	^{120}Nd	2.89	9.97×10^{-1}	1.59×10^{-7}	6.64		
	^{8}Be	^{116}Ce	5.99	7.47×10^{-12}	1.61×10^{-38}	37.63		
	^{12}C	^{112}Ba	17.87	1.60×10^{-15}	3.28×10^{-22}	21.33		
	^{16}O	^{108}Xe	28.45	3.89×10^{-18}	1.14×10^{-21}	20.78		
	^{20}Ne	^{104}Te	36.77	7.59×10^{-22}	6.77×10^{-26}	25.01		
	^{24}Mg	^{100}Sn	49.70	7.64×10^{-20}	3.30×10^{-18}	17.32		
	^{28}Si	^{96}Cd	56.23	4.68×10^{-23}	1.30×10^{-22}	21.73		

TABLE I. (*Continued*).

Parent nucleus	Emitted cluster	Daughter nucleus	Q value (MeV)	Preformation probability P_0	Decay constant λ (s^{-1})	$\log_{10} T_{1/2}^{cal}$ (s) Present	Ref. [9]	Ref. [10]
^{126}Sm	^{4}He	^{122}Nd	2.65	9.98×10^{-1}	1.27×10^{-9}	8.74		
	^{8}Be	^{118}Ce	4.52	2.17×10^{-12}	1.83×10^{-54}	53.58		
	^{12}C	^{114}Ba	15.92	5.77×10^{-21}	8.58×10^{-33}	31.91		
	^{16}O	^{110}Xe	26.65	1.09×10^{-23}	6.52×10^{-31}	30.03		
	^{20}Ne	^{106}Te	34.69	4.59×10^{-28}	3.76×10^{-35}	34.26		
	^{24}Mg	^{102}Sn	47.66	9.39×10^{-26}	1.51×10^{-26}	25.66		
	^{28}Si	^{98}Cd	56.95	2.74×10^{-26}	5.29×10^{-25}	24.12		
^{128}Sm	^{4}He	^{124}Nd	3.22	9.98×10^{-1}	2.09×10^{-6}	5.52		
	^{8}Be	^{120}Ce	4.47	2.02×10^{-12}	3.33×10^{-55}	54.32		
	^{12}C	^{116}Ba	14.87	1.44×10^{-23}	1.17×10^{-38}	37.77		
	^{16}O	^{112}Xe	24.83	4.04×10^{-33}	9.83×10^{-43}	41.85		
	^{20}Ne	^{108}Te	33.04	2.95×10^{-38}	6.82×10^{-48}	47.01		
	^{24}Mg	^{104}Sn	46.12	2.46×10^{-35}	1.51×10^{-37}	36.66		
	^{28}Si	^{100}Cd	54.91	2.63×10^{-36}	6.98×10^{-37}	36.00	25.4[c]	
^{128}Gd	^{4}He	^{124}Sm	3.70	3.96×10^{-1}	3.67×10^{-4}	3.28		
	^{8}Be	^{120}Nd	6.12	1.27×10^{-2}	2.00×10^{-31}	30.54		
	^{12}C	^{116}Ce	17.51	7.73×10^{-6}	1.55×10^{-15}	14.65		
	^{16}O	^{112}Ba	28.67	4.30×10^{-10}	1.63×10^{-15}	14.63		
	^{20}Ne	^{108}Xe	36.78	1.14×10^{-15}	2.93×10^{-22}	21.37		
	^{24}Mg	^{104}Te	50.02	3.27×10^{-19}	7.05×10^{-20}	18.99		
	^{28}Si	^{100}Sn	63.03	1.29×10^{-16}	6.84×10^{-13}	12.01		
^{130}Gd	^{4}He	^{126}Sm	4.16	3.89×10^{-1}	1.94×10^{-2}	1.55		
	^{8}Be	^{122}Nd	6.37	1.57×10^{-2}	7.02×10^{-28}	26.99		
	^{12}C	^{118}Ce	16.50	1.08×10^{-5}	1.51×10^{-18}	17.66		
	^{16}O	^{114}Ba	27.18	7.74×10^{-10}	7.58×10^{-18}	16.96		
	^{20}Ne	^{110}Xe	35.44	2.85×10^{-15}	4.34×10^{-24}	23.20		
	^{24}Mg	^{106}Te	48.48	2.21×10^{-20}	2.00×10^{-22}	21.54		
	^{28}Si	^{102}Sn	61.42	1.52×10^{-16}	5.70×10^{-16}	15.08		
^{132}Gd	^{4}He	^{128}Sm	3.90	3.76×10^{-1}	1.21×10^{-4}	3.76		
	^{8}Be	^{124}Nd	6.65	2.07×10^{-2}	2.33×10^{-26}	25.47		
	^{12}C	^{120}Ce	16.19	1.98×10^{-5}	4.76×10^{-19}	18.16		
	^{16}O	^{116}Ba	25.84	1.46×10^{-9}	4.36×10^{-20}	19.20		
	^{20}Ne	^{112}Xe	33.36	5.64×10^{-15}	2.73×10^{-27}	26.40		
	^{24}Mg	^{108}Te	46.57	9.47×10^{-21}	3.36×10^{-25}	24.31		
	^{28}Si	^{104}Sn	59.62	7.18×10^{-20}	7.75×10^{-19}	17.95		

[a]Masses are from Tachibana *et al.* [32] and Wapstra *et al.* [32].
[b]Masses are from Masson *et al.* [32] and Wapstra *et al.* [32].
[c]Masses are from Spanier *et al.* [32] and Wapstra *et al.* [32].

in general, the probability P_0 decreases as the size of the cluster increases. The nuclear shell structure effects are also demonstrated in P_0 by its being larger for clusters referring to doubly closed shell ^{100}Sn daughter (refer to ^{8}Be and ^{16}O clusters being preformed with almost largest P_0 values, respectively, in $^{108}_{54}$Xe and $^{116}_{58}$Ce parents). Notice, how ^{16}O cluster preformation probability increases as it approaches the ^{100}Sn daughter. The same is true of other clusters referring to the doubly closed ^{100}Sn or its neighboring daughter. In other words, the shell structure effects are evident in these plots in terms of the minima (largest P_0) or coming down of the graph of one cluster with respect to another.

Finally, the calculated decay half-lives, preformation probabilities P_0 and Q values are presented in Table I for various clusters. The calculations for Ba isotopes are given in Ref. [3], which together with Table I give a complete picture of the region studied here. The other model calculations are also shown in Table I for comparisons, where ever available [9,10]. We notice that our calculations here for the neutron-deficient parents match with other available calculations [9,10] as good as in the case of earlier neutron-rich radioactive or "stable" parents [2,16]. The agreement is very good in some cases (like ^{16}O decay of ^{118}Ce) but very bad in other cases (like ^{16}O decay of ^{122}Ce). Specifically, for the only observed ^{12}C decay of ^{114}Ba, our calculations [3] predict $T_{1/2} \approx 10^5$ s where as the other calculations [9,10] predict $T_{1/2} \approx 10^7$–10^8

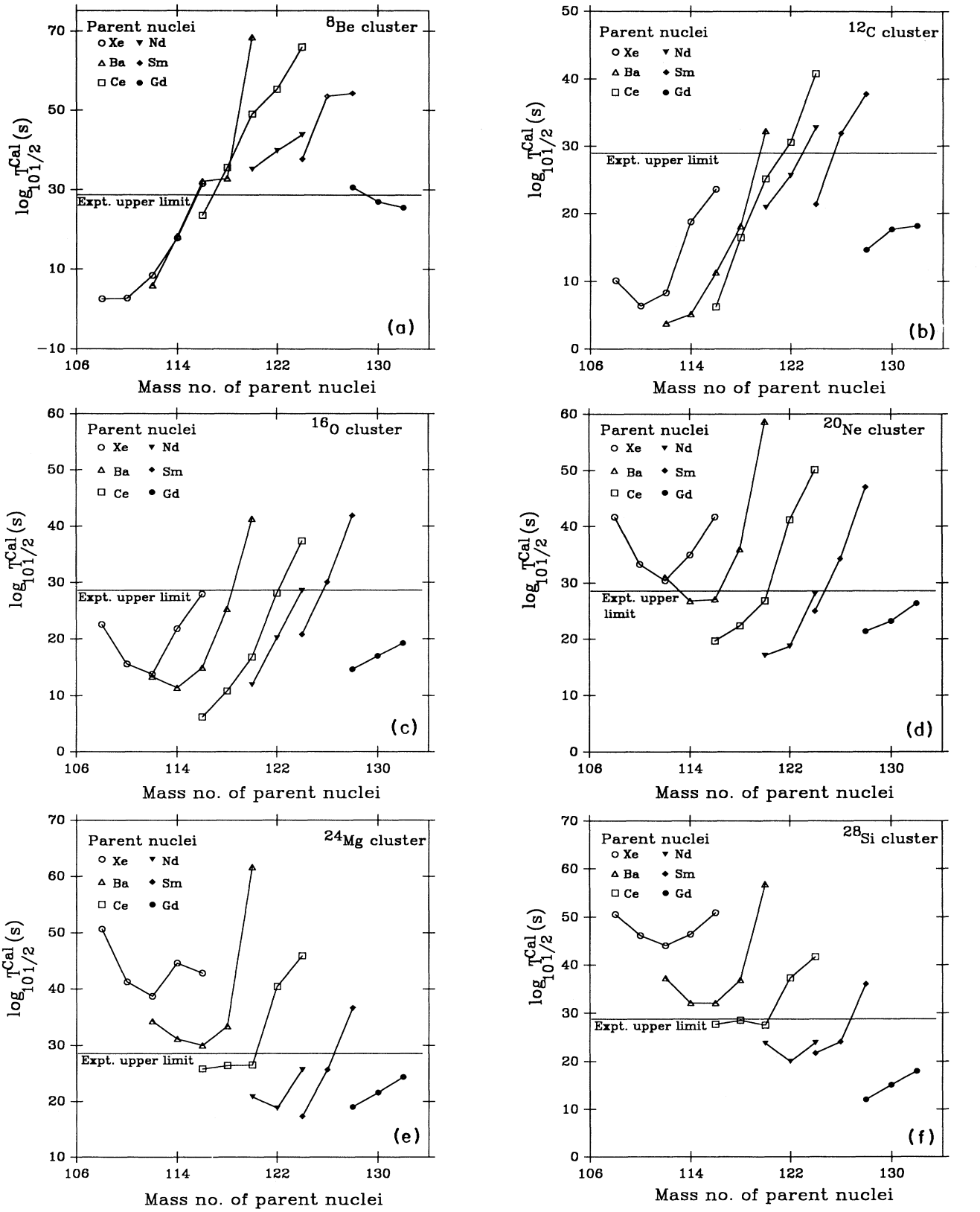

FIG. 5. (a) Logarithm of calculated half-lives vs mass of the parent nuclei $^{108-116}$Xe, $^{112-120}$Ba, $^{116-124}$Ce, $^{120-124}$Nd, $^{124-128}$Sm, and $^{128-132}$Gd, for ^{8}Be cluster. The results of calculation for Ba-isotopes are from Ref. [3]. The limit of present experiments is also shown. (b) Same as in (a), but for ^{12}C cluster. (c) Same as in (a), but for ^{16}O cluster. (d) Same as in (a), but for ^{20}Ne cluster. (e) Same as in (a), but for ^{24}Mg cluster. (f) Same as in (a), but for ^{28}Si cluster.

s; ours being much closer to experiments [5] [$T_{1/2}^{exp}(^{12}C) \approx 1.7 \times 10^4$ s]. All these calculations, however, depend strongly on the Q values used for calculating the penetrabilities P. Notice that in our case, the role of Q values (through the use of binding energies) also come in the calculation of preformation factor P_0.

Very recently,[3] a microscopic calculation [8] based on large single-particle basis and pairing two-body interaction has also become available for the cluster preformation factor P_0 in nuclei of the region under investigation. For the only calculation made for ^{12}C decay of ^{114}Ba, these authors [8] obtain $P_0 = 1.8 \times 10^{-7}$ which, for a similar Q value, compared nicely with our calculation [3] of $P_0 = 4.08 \times 10^{-8}$. As already stated in the introduction, the calculated half-lives in two models also agree within less than one order of magnitude.

Table I also shows that all the parents studied here (plus the Ba isotopes studied in Ref. [3]) are α emitters, and keeping in mind that the model of Malik and Gupta underestimates the α decay half-lives, all the calculated decay half-lives here lie below the present upper limit of experiments. The most probable (shortest $T_{1/2}$) α emitter is $^{108}_{54}$Xe, since its daughter $^{104}_{52}$Te$_{52}$ lies closest to the doubly magic $Z = N = 50$ shells. Perhaps, the α decay of $^{104}_{52}$Te parent (not studied here) will be even more probable, since the daughter will then be the doubly magic $^{100}_{50}$Sn nucleus itself. It is also evident from Table I that heavier deformed parents (like Sm or Gd) tend to become as good α emitters as the lighter parents like Xe or Ba. The same is true of heavier-cluster decays, up to ^{16}O, which is depicted in Figs. 5(a) to 5(c). We notice from Figs. 5(a), 5(b), and 5(c), respectively, that ^{8}Be cluster from $^{108-114}$Xe, ^{112,114}Ba, ^{116}Ce, and ^{130,132}Gd parents, ^{12}C from $^{108-116}$Xe, $^{112-118}$Ba, $^{116-120}$Ce, ^{120,122}Nd, ^{124}Sm, and $^{128-132}$Gd parents, and ^{16}O from $^{108-116}$Xe, $^{112-118}$Ba, $^{116-122}$Ce, $^{120-124}$Nd, ^{124}Sm, and $^{128-132}$Gd parents are the possible measurable cases with the present experimental methods. For clusters heavier than ^{16}O [Figs. 5(d) to 5(f)], the heavier parents are shown to decay more favorably (shorter $T_{1/2}$ values). Specifically, ^{20}Ne cluster decays of ^{114,116}Ba, $^{116-120}$Ce, $^{120-124}$Nd, ^{124}Sm, and $^{128-132}$Gd parents [Fig. 5(d)], ^{24}Mg decays of $^{116-120}$Ce, $^{120-124}$Nd, ^{124,126}Sm, and $^{128-132}$Gd parents [Fig. 5(e)], and ^{28}Si decays of $^{116-120}$Ce, $^{120-124}$Nd, ^{124,126}Sm, and $^{128-132}$Gd [Fig. 5(f)] parents, are predicted to lie below the upper limit of present experiments. Apparently, all these results fit nicely with the known fact that, being the still heavier nuclei, the radioactive parents are not only the best α emitters, but also the best heavy-cluster emitters. The interesting result here is that $^{108-114}$Xe, $^{112-116}$Ba, and ^{116,118}Ce are also predicted to be very good α emitters, as well as emitters of ^{8}Be, ^{12}C, and/or ^{16}O clusters. Similar to that for radioactive parents [16], the α-decay probabilities in this region of nuclei are also much larger (shorter $T_{1/2}$) than the heavy-cluster decay probabilities.

The dominance of $^{100}_{50}$Sn daughter is also evident in Figs. 5(a) to 5(f) for the heavier cluster decays. The emission of $^8_4$Be from $^{108}_{54}$Xe [Fig. 5(a)], $^{12}_6$C from $^{112}_{56}$Ba [Fig. 5(b)], $^{16}_8$O from $^{116}_{58}$Ce [Fig. 5(c)], $^{20}_{10}$Ne from $^{120}_{60}$Nd [Fig. 5(d)], $^{24}_{12}$Mg from $^{124}_{62}$Sm [Fig. 5(e)], and $^{28}_{14}$Si from $^{128}_{64}$Gd [Fig. 5(f)] are shown to be the most probable ones (smallest $T_{1/2}$ values). These are all $A_2 = 4n$, $Z_2 = N_2$ (α nuclei) cluster decays of $N = Z$ parents. Table I shows that for a given cluster decay, of all the parents, the Q value for the $N = Z$ parent is also the largest. This establishes that the ^{100}Sn daughter is associated with the $A_2 = 4n$, $Z_2 = N_2$ (α nuclei) cluster decays, and is referred to as Sn radioactivity. This new radiactivity is most probable for the $N = Z$ parents. Such a result is further strengthened when we study, in the following subsection, the $A_2 = 4n + 2$ cluster-decays.

B. $A_2 = 4n + 2$ cluster decays

As already pointed out above, Fig. 1 shows the potential energy minima at $A_2 = 4n + 2$ clusters for $N \gg Z$ parents only. Then, Table I and the GN plots in Fig. 3 show that, though the Q values for $A_2 = 4n + 2$ clusters are of the same order as for their neighbors ($A_2 = 4n$), the calculated $T_{1/2}$ values are always very large, i.e., beyond the present day experiments. For this reason we have not plotted the calculations for $A_2 = 4n + 2$ in any other graph. Hence, $A_2 = 4n+2$ cluster-decays of all the parents studied here and in Ref. [3], are far less favorable than the $A_2 = 4n$ cluster decays.

IV. SUMMARY AND CONCLUSIONS

We have presented the cluster-decay calculations for the even-even neutron-deficient $^{108-116}$Xe, $^{116-124}$Ce, $^{120-124}$Nd, $^{124-128}$Sm, and $^{128-132}$Gd parents, which combined with results of $^{112-120}$Ba from Ref. [3] constitute the region of possible $^{100}_{50}$Sn-radioactivity. The calculations are based on the well studied preformed cluster model (PCM) of Malik and Gupta.

We find that all the parents studied are good α emitters. For the heavy cluster decays, the systematics of calculated $T_{1/2}$ values fit nicely with the known properties of radioactive nuclei being as best α and heavy-cluster emitters. The $^{108-114}$Xe, $^{112-116}$Ba, and ^{116,118}Ce are predicted to be very good emitters of not only the α particle, but also the heavy ^{8}Be, ^{12}C, and/or ^{16}O clusters. In general, the $A_2 = 4n$, $Z_2 = N_2$ clusters are predicted to be far more probable than the $A_2 = 4n+2$ clusters. Furthermore, $A_2 = 4n$, $Z_2 = N_2$ (α nuclei) cluster decays of the $Z = N$ parents are predicted to be the most probable cases for measurements. This refers to clusters from ^{8}Be to ^{28}Si nuclei with $^{100}_{50}$Sn daughter, called Sn radioactivity. Hence, we have established here that Sn radioactivity is associated with the emission of $A_2 = 4n, Z_2 = N_2$ (α-nuclei) clusters, whereas it is known [16] that the already measured Pb radioactivity prefers the $A_2 \neq 4n$, $N_2 > Z_2$ clusters.

The nuclear structure effects of proximity potential or binding energies (shell effects) are shown to be contained in the GN plots, since all the plots deviate from straight

[3]See footnote 1.

lines and have different slopes and intercepts. The associated cluster preformation probability P_0 show the (doubly) closed shell effects of $^{100}_{50}$Sn daughter interms of its value becoming maximum or rising suddenly (refers to minima or coming down of the $-\log_{10} P_0$ vs parent mass A graphs). This happens for $A_2 = 4n$, $Z_2 = N_2$ (α nuclei) clusters emitted from $Z = N$ parents. Also, the P_0 values for α decay are the largest for all parents.

[1] R. K. Gupta, in Proceedings of the 5th International Conference on Nuclear Reaction Mechanisms, 1988, Varenna, Italy, edited by E. Gadioli (Ricerca Scientifica Educazione Permanente, Italy, in press), p. 416; S. S. Malik, S. Singh, R. K. Puri, S. Kumar, and R. K. Gupta, Pramana J. Phys. **32**, 419 (1989).

[2] R. K. Gupta, S. Singh, R. K. Puri, and W. Scheid, Phys. Rev. C **47**, 561 (1993).

[3] S. Kumar and R. K. Gupta, Phys. Rev. C **49**, 1922 (1994).

[4] Yu. Ts. Oganessian *et al.*, JINR, Dubna, Report No. E7-93-57, 1993.

[5] A. Guglielmetti, B. Blank, R. Bonetti, Z. Janas, H. Keller, R. Kirchner, O. Klepper, A. Piechaczek, A. Plochocki, G. Poli, P. B. Price, E. Roeckel, K. Schmidt, J. Szerypo, and A. J. Westphal, Nucl. Phys. A (to be published).

[6] S. S. Malik and R. K. Gupta, Phys. Rev. C **39**, 1992 (1989).

[7] R. Blendowske, T. Fliessback, and H. Walliser, Nucl. Phys. **A464**, 75 (1987).

[8] D. S. Delion, A. Insolia, and R. J. Liotta, J. Phys. G **20**, 1483 (1994).

[9] D. N. Poenaru, W. Greiner, and R. Gherghescu, Phys. Rev. C **47**, 2030 (1993).

[10] G. Shanmugam, G. M. Carmel-Vigila-Bai, and G. Suresh, DAE Symposium on Nuclear Physics (India) **36B**, 108 (1993).

[11] R. K. Puri, S. S. Malik, and R. K. Gupta, Europhys. Lett. **9**, 767 (1989).

[12] R. K. Gupta, W. Scheid, and W. Greiner, J. Phys. G **17**, 1731 (1991).

[13] S. Singh, R. K. Gupta, W. Scheid, and W. Greiner, J. Phys. G **18**, 1243 (1992).

[14] R. K. Gupta, S. Singh, R. K. Puri, A. Sandulescu, W. Greiner, and W. Scheid, J. Phys. G **18**, 1533 (1992).

[15] S. Kumar and R. K. Gupta, Int. J. Mod. Phys. E **3**, 195 (1994).

[16] R. K. Gupta and W. Greiner, Int. J. Mod. Phys. E **3**, 335 (1994, Supp.).

[17] B. Buck, C. B. Dover, and J. P. Vary, Phys. Rev. C **11**, 1803 (1975); B. Buck and A. C. Merchant, *ibid.* **39**, 2097 (1989).

[18] J. Cseh, Phys. Lett. B **281**, 173 (1992); G. Lavai, J. Cseh, and W. Scheid, Phys. Rev. C **46**, 548 (1992).

[19] J. Cseh, R. K. Gupta, and W. Scheid, Phys. Lett. B **299**, 205 (1993).

[20] R. K. Gupta, W. Scheid, and W. Greiner, Phys. Rev. Lett. **35**, 353 (1975).

[21] J. A. Maruhn and W. Greiner, Phys. Rev. Lett. **32**, 548 (1974).

[22] D. R. Saroha and R. K. Gupta, J. Phys. G **12** 1265 (1986).

[23] S. S. Malik, N. Malhotra, D. R. Saroha, and R. K. Gupta, International Centre for Theoretical Physics, Trieste, Italy, Report No. IC/86/128, 1986 (unpublished).

[24] G. Süssmann, Z. Phys. A **274**, 145 (1975).

[25] J. Blocki, J. Randrup, W. J. Swiatecki, and C. F. Tsang, Ann. Phys. (N.Y.) **105**, 427 (1977).

[26] H. Kröger and W. Scheid, J. Phys. G **6**, L85 (1980).

[27] S. Kumar, Ph.D. thesis 1993, Panjab University, Chandigarh, India.

[28] R. K. Gupta, *Frontier Topics in Nuclear Physics,* NATO Advanced Study Institute, edited by W. Scheid and A. Sandulescu (Plenum, New York, 1993).

[29] G. A. Pik-Pichak, Yad. Fiz. **44**, 1421 (1986) [Sov. J. Nucl. Phys. **44**, 923 (1986)].

[30] D. N. Poenaru, M. Ivascu, A. Sandulescu, and W. Greiner, Phys. Rev. C **32**, 572 (1985).

[31] R. K. Gupta, Fiz. Elem. Chastits At. Yadra **8**, 717 (1977) [Sov. J. Part. Nucl. **8**, 289 (1977)].

[32] P. E. Haustein, At. Data Nucl. Data Tables **39**, 185 (1988).